J. Phys.: Condens. Matter 7 (1995) 8197–8210. Printed in the UK

LNF-95/013

The influence of interstitial solutions (H, N) on the cerium electronic state in Ce–Fe intermetallic compounds: an x-ray absorption spectroscopy (XAS) study

Jesús Chaboy†, Augusto Marcelli‡ and Latchezar Bozukov§

Instituto de Ciencia de Materiales de Aragón, CSIC–Universidad de Zaragoza, 50009 Zaragoza, Spain

‡ INFN, Laboratori Nazionali di Frascati, Casella Postale 13, 00044 Frascati, Italy

§ Department of Solid State Physics, Faculty of Physics, Sofia University, 1126 Sofia, Bulgaria

Received 10 March 1995

Abstract. We present an x-ray absorption spectroscopy (XAS) investigation performed at the L edges of the rare earth and at the K edge of iron in the R–Fe intermetallic compounds $(La,Ce)_2Fe_{14}BH_x$ and $Ce_2Fe_{17}(H,N)_x$, to elucidate the role of the interstitial doping on the electronic and magnetic properties of these systems. Comparison with x-ray circular magnetic dichroism (XCMD) experiments has been carried out to clarify the localization of 4f magnetic moment at the Ce sites upon hydriding. Both XAS and XCMD results evidence the interplay between the structural and magnetic changes that are associated with the modification of the hybridization between the Fe(3d) and Ce(5d) bands.

1. Introduction

Since 1969 when Zijlstra and Westendorp reported the first observations about the ability of $SmCo_5$ to absorb large quantities of H_2 in a reversible way [1], a large body of research has been devoted to hydrogen absorption by intermetallic materials. As well as hydrogen being introduced by inadvertence in the pioneer studies subsequent interest was centred on the technological application of these materials [2]. Actually, it has been found that most of the members of the large group of intermetallic compounds formed among rare earths, R, and elements of the d transition series, M, can form stable hydrides and, very often, hydrogen absorption leads to strong changes of the macroscopic structural and magnetic properties of these materials [2–6]. Therefore, nowadays these studies have turned not only to the understanding of the mechanism responsible for hydrogen absorption by intermetallic compounds but also to ascertaining its effect on their magnetic, structural and electronic properties.

The interest has been recently renewed since the discovery of the $R_2Fe_{14}B$ materials [7, 8]. The ternary compound $Nd_2Fe_{14}B$ exhibits superior high-performance permanent-magnet properties and economic advantages over the earlier Sm–Co materials. However, the range of temperature in which these new alloys allow technological applicability is strongly limited because ordering temperatures, T_c, are sufficiently low to render them unsuitable for some applications [9–11]. This characteristic is shared by all the known R–Fe binary alloy compounds, whose Curie temperatures are rather low [12–14]. The origin of the peculiar behaviour of T_c is a matter of controversy. Several effects have been addressed

0953-8984/95/428197+14$19.50 © 1995 IOP Publishing Ltd

as responsible for this anomalous behaviour: the more localized character of Fe moments as compared to Co and Ni moments [12]; the peculiar sensitivity of the Fe–Fe exchange interactions to the Fe–Fe separation [15, 16]; local environment effects determining the molecular field coefficient, n_{FF}, that describes the Fe–Fe exchange interactions [16, 17]; and the role of spin fluctuations in T_c in itinerant electron systems [18].

Hydrogen absorption is one of the most notable mechanisms able to achieve a higher magnetic ordering temperature in these systems. The interstitial solution of H atoms leads to both an increase in the crystal cell volume, without a change in the crystal structure, and a rise of T_c. In the $R_2Fe_{14}BH_x$ series the relative volume expansion, $\Delta V/V$, varies between 2% and 6% and the increase on T_c varies between 40 and 50 K depending on the nature of the rare earth [19–23]. This behaviour was interpreted in terms of the modification of the shortest Fe–Fe distances that according to the Slater–Néel curve can give rise to antiferromagnetic exchange interactions [24]. These findings have stimulated attempts to improve the magnetic properties of other R–Fe alloys, such as the R_2Fe_{17} intermetallics, by using hydrogen absorption, that raises T_c by around 200 K in this series [25–28]. More recently, these studies have been extended to other interstitial solutions such as C and N atoms. It has been found that in the R_2Fe_{17} intermetallics, interstitial C raises the Curie temperature up to 200 K [29–31], while the effect of nitrogen is even greater, producing increases of about 400 K [32–34].

One of the most fascinating results obtained by studying the interstitial doping in R–3d intermetallics is associated with the possibility of inducing a change of valency on Ce atoms [35]. Indeed, such a behaviour should open a new route to develop a net Ce 4f magnetic moment in these materials. However, how the electronic structure of Ce ions in $Ce_2Fe_{14}B$ and Ce_2Fe_{17} systems is modified upon hydrogen (nitrogen) absorption is nowadays a matter of controversy. Severals authors have claimed for the existence of a Ce^{4+} to Ce^{3+} transition, i.e., from non-magnetic to magnetic configurations, taking place upon interstitial doping. This assignment has been proposed on the basis of the anomalous relative volume increase for the cerium compounds, that is significantly larger than those observed for the rest of the series [28, 35–43]. The relative volume increase upon hydrogen uptake, $\Delta V/V$, is found to be 5.5% and 6.2% for $Ce_2Fe_{14}B$ and $Pr_2Fe_{14}B$ compounds, respectively [21]. A similar trend has been also observed in the case of the $R_2Fe_{17}H_x$ series, in which $\Delta V/V$ is 5.3% and 4.4% for Ce and Pr, respectively [36]. Moreover, in the case of nitrogen absorption, this effect is even greater, being $\Delta V/V = 8.8\%$ and between 5.8 and 7.4% for Ce_2Fe_{17} and Pr_2Fe_{17} compounds respectively [34, 36, 37, 38]. However, although an earlier neutron diffraction investigation performed on $Ce_2Fe_{14}B$ and its hydride derivatives reported the development of a 2.2 μ_B magnetic moment at the Ce 4g site for deuterated samples [35], this assignment has not been confirmed either by x-ray photoelectron spectroscopy [39] nor by x-ray absorption spectroscopy [44, 45]. However, qualitative support of the neutron diffraction results has been found from recent analyses of XAS data [46]. Moreover, while in the case of the $CeFe_2$ system it is well established that Ce ions develop a magnetic moment of 4f origin upon hydrogen absorption [45, 47, 48], in the case of Ce_2Fe_{17}, $Ce_2Fe_{14}B$ and their hydrides, XAS experiments do not support the interpretation based on the interplay between cerium valency and hydrogen absorption [44, 45, 49–51].

In this work, we report an extensive x-ray absorption spectroscopy (XAS) study performed at the rare earth L edges and at the Fe K edge in the case of $La_2Fe_{14}B$, $Ce_2Fe_{14}B$ and Ce_2Fe_{17} systems and their hydride derivatives. The aim of this work is to establish the modification of the electronic structure of Ce upon hydrogen absorption. This investigation has been extended to the study of the Ce_2Fe_{17} system upon nitrogen uptake. The valency state of cerium has been investigated by x-ray absorption near-edge structure (XANES) at

the Ce L_3 edge. In addition, measurements of the cerium L_1 edge and Fe K edge XANES spectra have been performed to determine the modification of the local and partial density of states around the Fermi energy induced by interstitial doping. Such combined analysis shows electronic localization phenomena that address the change in the magnetic properties of the systems upon hydriding to the modification of the 3d(Fe)–5d(R) hybridization. To discuss the dynamics of the Ce electronic state upon hydrogen (nitrogen) absorption in these iron-rich intermetallic compounds, XAS results are compared to x-ray circular magnetic dichroism (XCMD) experiments recently published [49, 52].

2. Experimental set-up

Samples were prepared by arc-melting the starting elements (purity 99.9%) under purified Ar atmosphere. Both phase and structural analysis were performed on a standard x-ray diffractometer. The hydrogen (nitrogen) absorption–desorption properties were established according to the standard methods [20, 28, 32].

XAS experiments have been performed at the Fe K edge and at the $L_{1,3}$ edges of La and Ce in the case of $(La, Ce)_2Fe_{14}BH_x$ and $Ce_2Fe_{17}(H, N)_x$ systems (x being the maximum gas content). Several samples were measured in different experimental runs at the PULS synchrotron radiation facility of the Laboratori Nazionali di Frascati. The ADONE storage ring was operated at 1.5 GeV during dedicated beam time with an averaged current of 40 mA.

For these experiments fine powders of the material were homogeneously spread on an adhesive tape. Thickness and homogeneity of the samples were optimized to obtain the best signal to noise ratio using two layers of powdered material giving a total absorption jump, $\Delta\mu x$, ranging between 0.4 and 0.8 as a function of the absorption edge selected. Measurements were carried out at room temperature in the transmission mode, the x-ray radiation being monochromatized using a Si(111) channel-cut crystal. Both incident x-rays and three transmitted through the sample were monitored by using two independent ionization chambers with N_2–Ar flowing gas mixture optimized for each energy range.

The absorption spectra were analysed according to standard procedures [53]. The background contribution from lower-energy absorption edges, $\mu_B(E)$, was approximated according to the Victoreen rule and subtracted from the experimental spectrum, $\mu(E)$. Spectra were then normalized to the absorption coefficient at high energy to eliminate thickness dependence. The energy origin E_0, corresponding to the continuum threshold, was defined to be at the inflection point of the absorption edge.

3. Results and discussion

3.1. Fe K edge XANES spectra

The x-ray absorption spectrum is usually divided into three regions as a function of the kinetic energy of the photoelectron: the first part of the spectrum extending over about 10 eV, called the edge region; the region of the multiple scattering in the continuum, XANES, and the region of single scattering at higher energies, EXAFS. In the XANES and EXAFS regions, the photoelectron is scattered in real space by neighbouring atoms so that direct structural information, i.e., coordination geometry and bond angles, can be extracted from the absorption spectra, whereas the near-edge region of the spectrum carries information about the electronic state of the absorbing atom [54].

The normalized XANES spectra recorded at the Fe K edge in the case of $La_2Fe_{14}B$

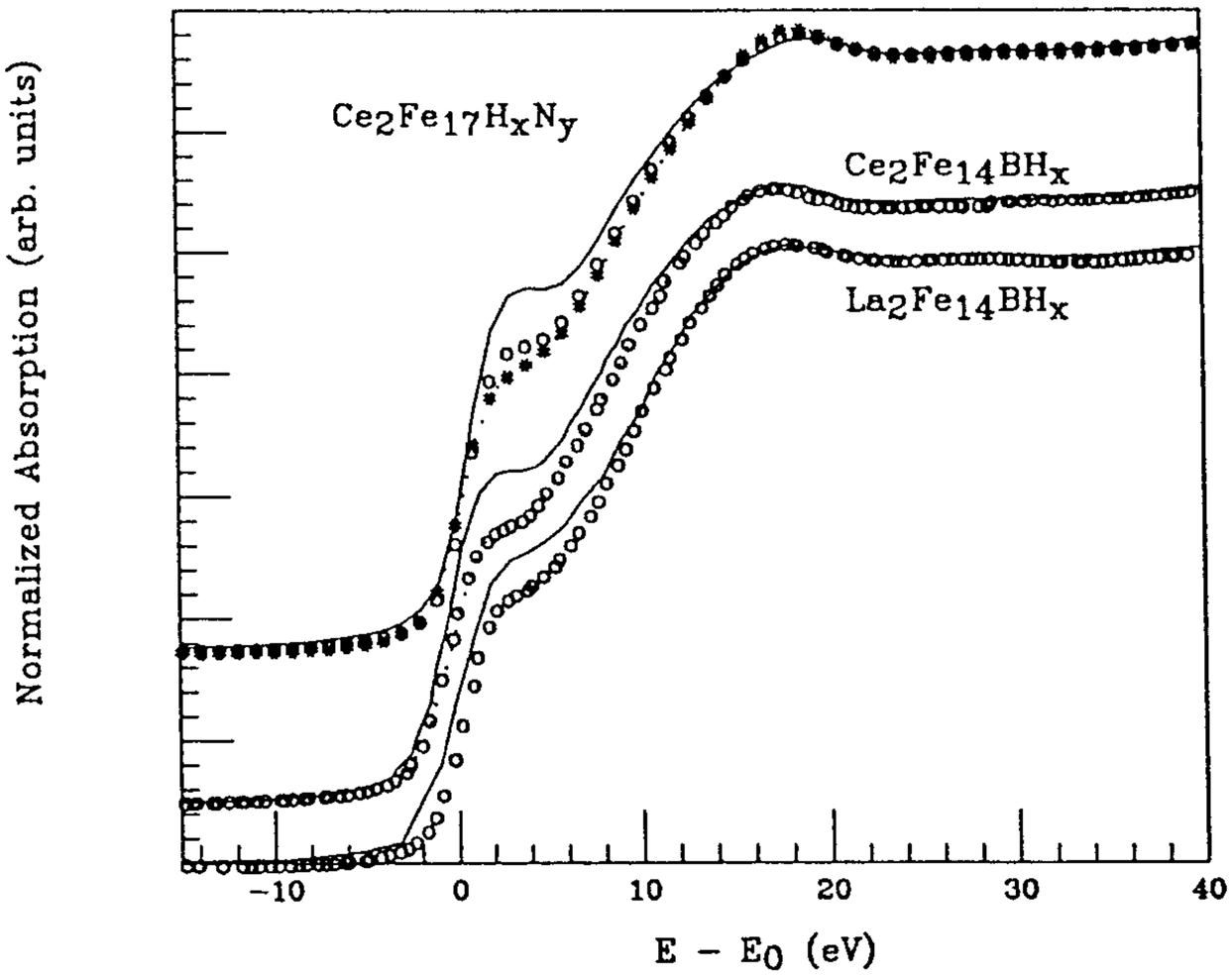

Figure 1. Comparison between the experimental XANES spectra at the Fe K edge in the case of $La_2Fe_{14}B$, $Ce_2Fe_{14}B$ and Ce_2Fe_{17} (solid) and their hydride derivatives. In the case of Ce_2Fe_{17} also the nitride $Ce_2Fe_{17}N_y$ is shown (*).

and its hydride derivative are compared in figure 1. The XANES spectrum of the parent compound is characterized by exhibiting a steplike feature at the edge, similar to that of iron metal. The origin of the feature has been successfully interpreted as due to the hybridization between the p–d conduction empty states at the Fermi level [54]. Hence, although in the K edge absorption a core electron is removed from the 1s shell and excited to a p symmetry final state, the existence of the p–d hybridization makes possible to probe, indirectly, the behaviour of the magnetic d states. Upon hydrogen absorption, no significant modification of the XANES resonances is detected, both in energy position and intensity, as expected because the crystal structure of the unhydrided parent compound is retained [22]. However, the differences found in the near-edge region of the absorption spectra corresponding to the $La_2Fe_{14}B$ and $La_2Fe_{14}BH_x$ compounds are noticeably strong at the Fe K absorption edge. Therefore, the impact of the hydrogen absorption in the crystal structure is rather small, whereas the large differences observed in the edge region address the presence of strong electronic effects induced on Fe atoms.

The present results show that the Fe K edge threshold is shifted towards higher energies upon H_2 uptake, and that the intensity of the shoulder-like feature at the edge decreases upon hydrogen absorption. The same behaviour is found in $Ce_2Fe_{14}B$ and Ce_2Fe_{17} compounds, as also shown in figure 1. Within our experimental resolution, in the case of Ce_2Fe_{17}, both effects are slightly larger for the nitrogen interstitial-doped compound as compared with the hydride derivative.

These results reveal the existence of a strong electronic perturbation on the Fe atoms driven by the interstitial doping. Indeed, the shift of the threshold towards higher energy for the interstitial doped compounds can be related to the shift of the Fermi level towards higher energy, while the decrease of the intensity of the shoulder-like resonance at the raising edge indicates that the density of empty p (d) states above the Fermi energy decreases upon H_2 (N) uptake. The origin of such a resonance is due to the large p–d hybridization of the conduction bands at the Fermi level, so that the photoelectron finds a large density of dipole-allowed delocalized p like final states. The observed reduction indicates that the local density of p(d) states, projected on the Fe sites, is reduced after the interstitial doping.

As a consequence, we can infer from XAS data that the Fermi level shifts towards higher energy and sites in a region with a lower density of states in the case of the hydride (nitride) derivatives.

Based on the above results a deeper insight into the origin of the modification of the magnetic properties induced by hydrogen (nitrogen) in these intermetallic compounds can be obtained. Indeed, upon hydrogen absorption, an increase of the magnetic moment of Fe atoms has been observed in all the R–Fe systems investigated to date. In contrast, an opposite behaviour is found for Co- and Ni-based compounds. Several mechanisms have been proposed to account for such a controversial behaviour. In the case of the $R_2Fe_{14}B$ series, Andreev *et al* [55] have proposed that hydrogen uptake leads to the formation of low-energy electron states which are filled by electrons coming from the 3d band. In this scheme, the increase in μ_{Fe} should be due to an increase of the splitting of the 3d band, acompanied by a decrease of the Fermi energy. Others authors have interpreted the increase of the Fe magnetic moment as due to the narrowing of the 3d band or to the weakening of the R–Fe hybridization upon gas uptake [4, 11].

However, the shift towards higher energy of the Fermi level observed by XANES rules out the hypothesis of a low-lying state formation upon interstitial doping. Moreover, this result cannot be understood taking into account, as the only responsible mechanism, a narrowing of the 3d band due to the cell expansion. In fact, it is necessary to consider that the 3d band becomes gradually filled upon H_2 uptake as earlier proposed by Kuijpers [56]. The Fe K edge XANES spectra show a similar trend of the Fermi level upon gas uptake in all the systems investigated, so that it sites in a lower-density-of-states (DOS) region independently of both the rare earth component (La,Ce), and the Fe concentration ($Ce_2Fe_{14}B$, Ce_2Fe_{17}). This result suggests the existence of an interplay between the charge-transfer effect and the decrease of the hybridization between the rare earth and the Fe conduction bands induced by the interstitial doping. In addition, the shift of the Fermi level in both $La_2Fe_{14}B$ and $Ce_2Fe_{14}B$ systems is similar, whereas the narrowing of the 3d band caused by the crystal cell expansion is expected to be larger for the Ce-based compound. Moreover, in the case of the Ce_2Fe_{17} derivatives, the shift of the Fermi level is lower than that found in the $R_2Fe_{14}BH_x$ compounds, whereas the crystal cell expansion is significantly larger. This last result is in agreement with the existence in the latter compounds of more conduction electrons available in the system after the gas absorption.

Finally, it is important to note that for similar hydrogen and nitrogen charging of the Ce_2Fe_{17} compound, while the observed shift of the threshold energy is identical, the decrease of the shoulder-like resonance at the rising edge is markedly larger in the nitride derivative. This result can be related to a larger decrease of the hybridization of the valency electrons of the rare earth with the 3d electrons of Fe atoms induced by nitrogen. As consequence, the broadening of the 3d band becomes smaller in $Ce_2Fe_{17}N_x$ than in $Ce_2Fe_{17}H_x$ and Ce_2Fe_{17}, enhancing the effective Coulomb repulsion and the band splitting, thus leading to a larger increase of the Fe 3d moment in the former compound.

3.2. L_3 edge XANES spectra: mixed-valency behaviour of cerium

Both $Ce_2Fe_{14}B$ and Ce_2Fe_{17} compounds present anomalously small cell parameters as compared with those of the rest of the respective series. Moreover, according to numerous experimental investigations, Ce atoms do not carry any magnetic moment of 4f origin [57, 58]. Upon hydrogen and nitrogen absorption, the Ce-based materials suffer the highest cell expansion in both $R_2Fe_{14}B$ and R_2Fe_{17} series, a trend that has been largely associated to the development of a localized magnetic moment at the Ce sites upon gas charging [28,

35–43]. However, previous XAS experiments performed at the Ce L_3 edge in the hydrides derivatives have shown the inadequacy of such a scheme [44, 45].

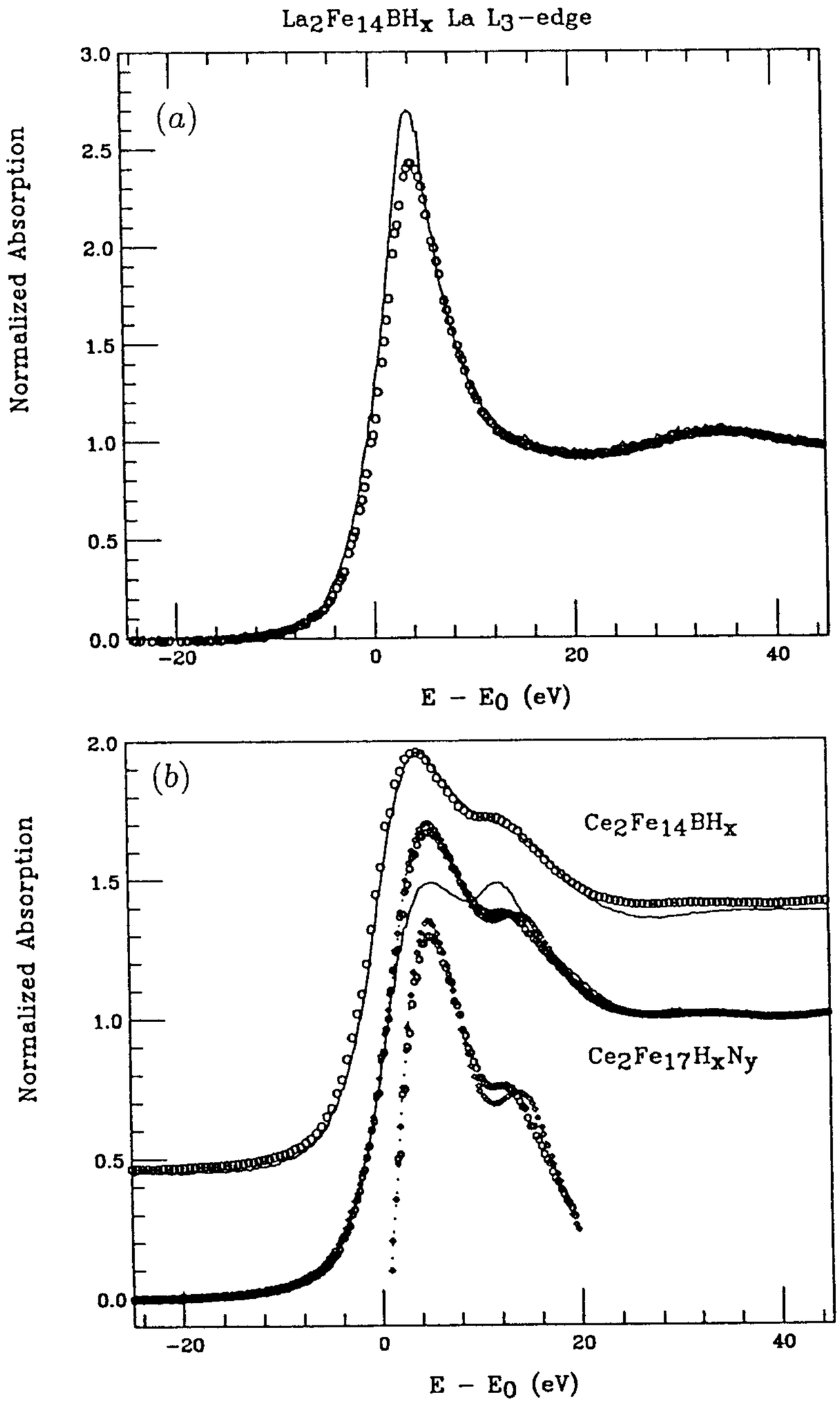

Figure 2. (a) Comparison between the La L_3 edge XANES spectra for $La_2Fe_{14}B$ (solid) and $La_2Fe_{14}BH_x$ (dots); (b) normalized Ce L_3 edge XANES spectra in the case of $Ce_2Fe_{14}B$ (solid) and its hydride derivative (dots), and Ce_2Fe_{17} (solid) $Ce_2Fe_{17}H_x$ (dots) and $Ce_2Fe_{17}N_x$ ($\diamond$). At the bottom, a magnified view of the edge region for both Ce_2Fe_{17} hydride and nitride derivatives is shown.

The absorption at the L_3 edge of the rare earth in these compounds constitutes a good challenge to investigate both the impact of the interstitial gas on the 5d band and the dynamics of the Ce electronic state. The possibility of probing directly the rare earth 5d band is of fundamental interest in the case of $La_2Fe_{14}B$ and $La_2Fe_{14}H_x$ compounds. Indeed, due to the absence of magnetic moment of 4f origin on the La atoms, the 5d magnetism is exclusively due to the hybridization of the 5d band with the 3d band of Fe. Hence, any modification of this 5d–3d hybridization, associated with the gas charging, should be reflected in the XANES absorption profile. The XANES spectra at the La L_3 edge in the

case of $La_2Fe_{14}B$ and its hydride derivative are shown in figure 2. They are characterized by exhibiting a pronounced peak at the absorption threshold, that corresponds to the atomic $2p \rightarrow 5d$ transition (white line). This behaviour is common to both rare earth vapours and metals, indicating that the 5d states retain their atomic character upon condensation. In the case of the hydride derivative, the white line shows two marked changes with respect to that of the unhydrided parent $La_2Fe_{14}B$: it becomes narrower and less intense; and, as in the case of the Fe K edge, the edge is shifted towards higher energy. The second effect reflects the existence of a shift of the Fermi level induced by the injection of more electrons to the conduction bands of the system. On the other hand, the narrowing of the white line profile reflects a higher localization of the 5d band at the La sites and, consequently, the weakening of the hybridizaton between the La 5d and Fe 3d bands. This picture is also supported by the decrease of the white line height upon hydrogen uptake, indicating the reduction of the d-symmetry empty states at the La sites, as expected if the 3d–5d overlap becomes smaller.

In the case of the Ce-based materials, namely $Ce_2Fe_{14}B$ and Ce_2Fe_{17}, the XANES spectra at the Ce L_3 edge show a characteristic double peak reflecting the existence of two configurations in the initial state, $4f^n$ and $4f^{n+1}$, as shown in figure 2. This peculiar profile is made by the superposition of the atomic $2p \rightarrow 5d$ transition for each ground state configuration, the white line corresponding to the $4f^{n+1}$ configuration shifted to lower energy with respect to that of the $4f^n$ one. Therefore, the study of the absorption spectra at the Ce L_3 edge provides an unique tool to determine the electronic state of Ce. In the case of the $Ce_2Fe_{14}B$ and Ce_2Fe_{17}, the XANES spectra indicate that Ce atoms present mixed-valency behaviour. The fractional occupancy of the 4f configurations in the initial state, i.e., the electronic valency, can be estimated through the deconvolution of the normalized XANES spectra [51].

The deconvolution of the L_3 absorption edge of cerium for $Ce_2Fe_{14}B$ and Ce_2Fe_{17} returns a valency of 3.22 and 3.33 respectively. Upon hydrogen absorption no modification of cerium valency is found for the $Ce_2Fe_{14}B$ compound. In contrast, both Ce_2Fe_{17} hydride and nitride exhibit a decrease of the Ce valency to 3.22 . Hence, the Ce mixed-valency behaviour is retained in all these systems, ruling out the possibility of the developing of a 4f magnetic moment induced by hydrogen (nitrogen) uptake. Our results demonstrate that the strong expansion of the crystal structure in both Ce-based compounds upon gas charging is not linked to the modification of the Ce electronic state. In addition, they constitute evidence of the weakening of the 3d–5d hybridization induced by both hydrogen and nitrogen absorption.

3.3. L_1 edge XANES spectra

The previous analyses of the Fe K edge, Ce and La L_3 edge XANES absorption spectra indicate that the gas charging modifies the overlapping between the conduction bands of both rare earth and Fe. An additional test of this effect can be obtained by tuning the energy of the absorption at the L_1 edge of the rare earth elements.

The spectral shape of the L_1 spectra in all the lanthanide metals exhibits a steplike rise of the absorption at the threshold. This feature reflects the p projected density of states in the band structure of the conduction electrons. In the case of rare earth vapours, such a structure is absent from the L_1 spectra because the atomic resonances corresponding to the one-electron transition s–p are very weak due to the small oscillator strengths of the s–p transitions [59, 60]. However, upon condensation into the metallic state, the L_1 spectra lose their atomic character completely and a shoulder-like feature appears [61]. This behaviour is the experimental evidence that the outer p symmetry orbitals are strongly hybridized with the

outer s and d symmetry orbitals in metals, reflecting the high density of empty 5d states via hybridization of the R(sp) and R(5d) empty states. Therefore, the modification of the width and intensity of the shoulder-like near edge structure is a fingerprint of hybridization changes of the outermost orbitals between the absorbing atom and the nearest neighbours. Actually, in the case of R–Fe intermetallic compounds, due to the strong hybridization between the rare earth 5d and Fe-3d orbitals, the study of the L_1 absorption spectra provides a unique insight to study the behaviour of the R(5d)–Fe(3d) hybridization upon gas charging.

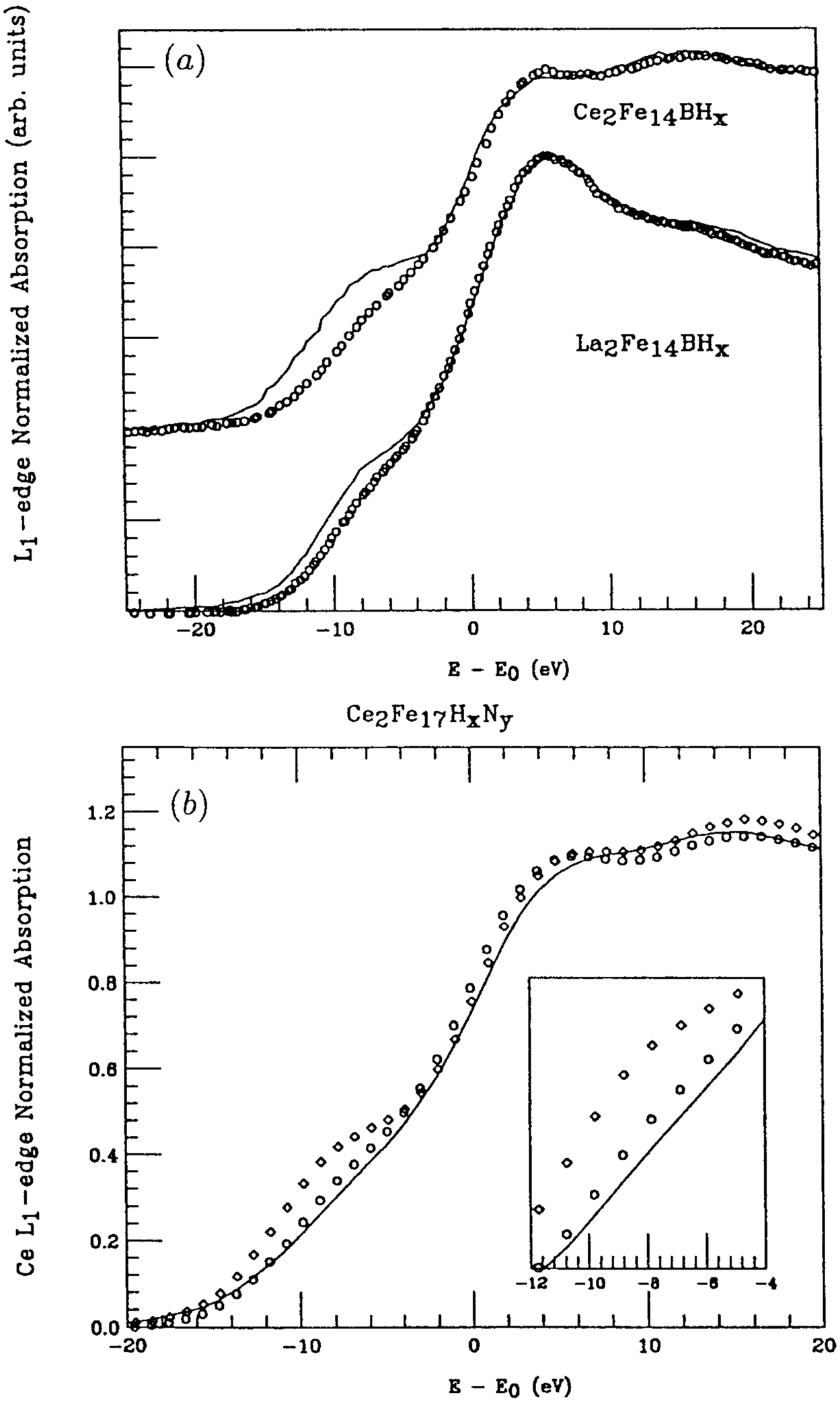

Figure 3. Comparison between the experimental XANES spectra at the rare earth L_1 edge in the case of (a) $La_2Fe_{14}B$ and $Ce_2Fe_{14}B$ (solid) and their hydride derivatives (dots); (b) Ce_2Fe_{17} (◇), $Ce_2Fe_{17}H_x$ (dots) and $Ce_2Fe_{17}N_x$ (solid). The inset reports the differences of the near edge region for the hydride and nitride derivatives.

Figure 3 shows the comparison of the XANES spectra at the La and Ce L_1 edge in both $La_2Fe_{14}B$ and $Ce_2Fe_{14}B$ and their hydride derivatives. In both cases, a reduction of the shoulder-like feature is induced by hydrogen absorption, indicating a more localized nature of the p–d orbitals of the rare earth, similar to the rare earth vapour case. This result

supports the hypothesis that a higher localization of the 5d band at the rare earth site takes place upon hydriding, as well as the concomitant reduction of the R(5d)–Fe(3d) overlap that determines the interplay between the two magnetic sublattices. We have to notice that the narrowing of the shoulder is greater in the $Ce_2Fe_{14}B$ hydride than in the $La_2Fe_{14}B$ one, addressing the anomalous volume expansion of the Ce-based hydride to a higher reduction of the R–Fe hybridization, rather than to a change of the cerium valency, which indeed is not detected in our experiments. Moreover, comparison of the Ce L_1 XANES spectra of Ce_2Fe_{17} and its hydride and nitride derivatives, shown in figure 3, exhibits a huge reduction of the edge feature upon gas charging, as in the $Ce_2Fe_{14}BH_x$ systems. This reduction is slightly larger for the nitride than for the hydride derivative, also in agreement with the higher volume expansion observed in the former compound.

3.4. XCMD study in $R_2Fe_{14}BH_x$ systems (R = La, Ce)

From the previous analyses of the XANES spectra we showed that the mechanism playing a major role in the modification of the electronic and magnetic properties of the $La_2Fe_{14}B$, $Ce_2Fe_{14}B$ and Ce_2Fe_{17} systems upon gas charging is mainly related to the change of the R–Fe hybridization. A further test can be achieved by analysing the x-ray circular magnetic dichroism (XCMD) at the rare earth L and at the Fe K absorption edges. Indeed, by recording the spin-dependent absorption cross-section it is possible to probe the spin polarization of the 5d empty states of the rare earth L_2 edge, and the 4p empty states of the Fe K edge [62]. The XCMD probe is of fundamental interest because it allows us to characterize magnetically the 5d states that mediate the 4f-3d exchange interaction, and thus the magnetic properties of the R–Fe intermetallic compounds.

Figure 4 shows the comparison of the La L_2 edge XCMD spectra for $La_2Fe_{14}B$ and its hydride derivative. The comparison performed at the iron K edge is also shown. The spin-dependent absorption coefficient has been obtained as the difference of the absorption coefficient $\mu_c = (\mu^- - \mu^+)$ for parallel, μ^+, and antiparallel, μ^-, orientation of the photon spin and the magnetic field applied to the sample. The L_2 absorption spectrum is sensitive to the $d_{3/2}$ final state density, and, due to the existence of spin–orbit coupling in the initial state, the XCMD spectra are directly related to the spin polarization of the final d states projected on the La site. This fact makes possible to relate the dichroic signal to the magnetic moment carried by the 5d electrons. Hence, according to Brouder and Hikam [63], the XCMD signal at the L_2 edge, defined as above, can be written as

$$\Delta\sigma_{L_2} = \frac{\sigma^-(\boldsymbol{B}) - \sigma^+(\boldsymbol{B})}{\sigma^+(\boldsymbol{B}) + \sigma^-(\boldsymbol{B})} = \frac{\sigma^{\uparrow}_{21/2} - \sigma^{\downarrow}_{21/2}}{2(\sigma^{\downarrow}_{21/2} + \sigma^{\uparrow}_{21/2})} \tag{1}$$

where $\sigma^{\uparrow(\downarrow)}_{2_j}$ holds for the reduced transition probability towards spins parallel (antiparallel) to the magnetization direction. Consequently, the analysis of the XCMD spectra would lead to a direct determination of the sign of the magnetic coupling between the La 5d and the Fe 3d spins. In the case of $La_2Fe_{14}B$ and its hydride derivative XCMD signals are negative at the L_2 edge, indicating that the dominant transitions are those towards spin 5d states antiparallel to the magnetization direction. The energy distance between the bonding and antibonding 3d–5d subbands is different for the two spin directions and therefore 3d–5d hybridization is different for the majority and minority spins [64], so that under the absence of localized 4f magnetic moments the occupancy of the spin down (minority) part of the 5d component is expected to exceed that of the spin up (majority) part that is hybridized to the majority spin Fe 3d band. Consequently there is a total 5d spin moment on the rare earth coupled antiferromagnetically to the Fe 3d moment.

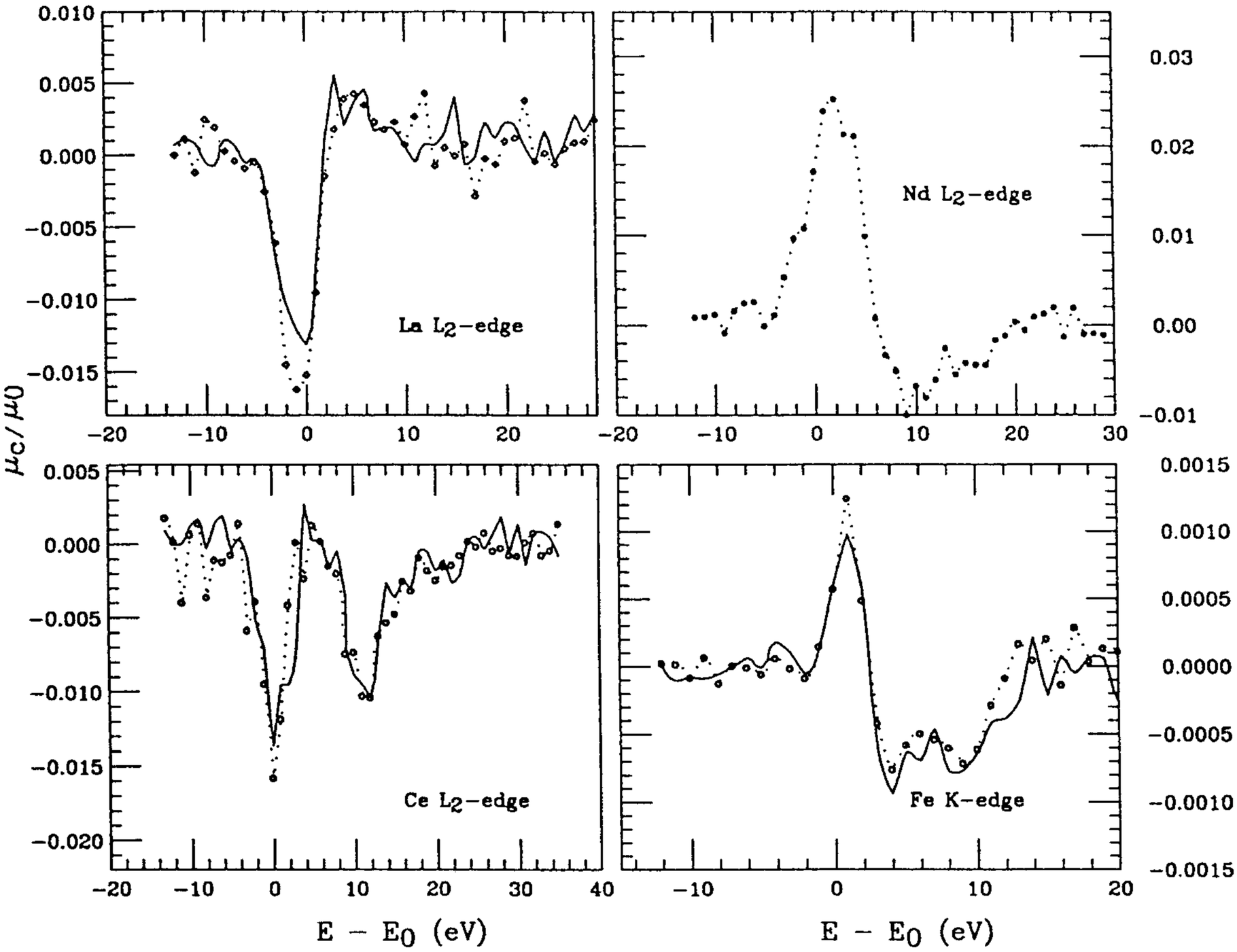

Figure 4. XCMD signals at the Fe K edge (bottom right) and La L_2 edge (top left) of $La_2Fe_{14}B$ (solid) and $La_2Fe_{14}BH_x$ (dots). Comparison is also shown for the XCMD signals at the Ce L_2 edge (bottom left) of $Ce_2Fe_{14}B$ (solid) and $Ce_2Fe_{14}BH_x$ (dots). The Nd L_2 edge XCMD signal of $Nd_2Fe_{14}B$ is also shown in the top right panel.

In the case of $La_2Fe_{14}B$, $Ce_2Fe_{14}B$ and their hydrides, XCMD spectra support the scheme above, indicating both the existence of an ordered net 5d magnetic moment at the La and Ce sites as well as its antiferromagnetic coupling to the Fe 3d magnetic moment, in agreement with the Campbell indirect exchange hypothesis [65]. Upon hydriding, the La L_2 edge XCMD signal of the $La_2Fe_{14}B$ increases with respect to that of the parent compound. According to Johanson's model, the reduction of the 5d–3d hybridization implies a further decrease of the 5d content in the bonding band, which is larger for the spin up component and consequently, the number of accessible spin up 5d states decreases more than that of the spin down states [64]. Within this framework and according to equation (1), if the H_2 uptake leads to the weakening of the 5d–3d hybridization the XCMD signal should increase, as experimentally confirmed by our data.

The XCMD signal at the Ce L_2 edge in $Ce_2Fe_{14}B$ and its hydride present a double-peak structure that resembles the existence of configurational mixing in the ground state, as in the case of polarization-averaged XAS spectra (see figure 3). Moreover, the sign of the XCMD is negative as for nonmagnetic rare earths [66]. In contrast, in magnetic rare earths the 4f states are split into the occupied states, occuring at about -7 eV below E_F, and those unoccupied above the Fermi level [67]. In these cases, although the number of empty spin up (majority) 5d states exceeds that of the minority spin above the Fermi level, the matrix elements for the transition to the spin down states are larger than to the spin up states because of the intra-atomic 4f–5d overlap [68–71]. As a consequence, the sign of the XCMD has to be positive, as shown in figure 4 for the case of $Nd_2Fe_{14}B$ [52]. Therefore, upon developing of a localized Ce 4f magnetic moment in the $Ce_2Fe_{14}B$ hydride, a change

of sign of the XCMD should be expected, contrary to the experimental result [49].

Finally, we briefly comment the behaviour of the XCMD signal at the Fe K edge in the case of $La_2Fe_{14}B$ and its hydride derivative. Both signals are almost identical to that of iron metal [52], and present a narrow positive peak, $\simeq$5 eV wide, followed by a broader negative signal. This profile has been accounted for in the case of Fe metal by considering the spin splitting of the final p-projected states at the Fe site and the hybridization of the 4p and 3d states, which modulates the weight of the spin-dependent absorption cross-section for transitions towards spin up (down) 4p states [63]. Furthermore, the sign of the XCMD signal at the Fe sites indicates that the majority of 4p spins are antiferromagnetically coupled to the 3d spins [63]. Despite the fact that the relationship between the XCMD signal at the K edge and the local magnetic moments is not well defined, being system dependent, the close similarity of the Fe K edge XCMD signals in these systems and that of iron metal may be interpreted as indicating that the impact of additional charge transfer from the rare earth to the conduction bands has no remarkable effect at the Fe sites. On this basis, the behaviour of the XCMD signal upon hydrogen absorption, showing the increase of the positive peak and the decrease of the intensity at depth, can be associated according to [63] to the enhancement of the Fe 3d magnetic moment [63, 76, 77].

3.5. Conclusions

The interpretation of the x-ray absorption spectra recorded at the rare earth $L_{1,3}$ edges and at the Fe K edge clarifies the origin of the magnetic changes occurring upon hydrogen (nitrogen) uptake in $R_2Fe_{14}B$ (R = La, Ce) and Ce_2Fe_{17} systems.

The analysis of the Fe K edge and rare earth L_1 XANES spectra shows the existence of strong electronic effects induced upon gas charging. The interplay between electronic charge transfer to the conduction bands and the weakening of the hybridization between the R 5d and the Fe 3d states is responsible for the enhancement of the Fe magnetic moment.

Contrary to previous assignments [28, 35–43], the mixed-valency behaviour of Ce, determined from the L_3 absorption XANES analysis, indicates that upon H_2 (N) uptake no development of a localized 4f magnetic moment takes place. A claim for the developing of 4f magnetic moment in Ce ions upon hydrogen uptake in these compounds has been proposed by establishing a parallel to the isostructural γ–α transition of Ce metal, that exhibits a $\simeq$16% volume collapse and the extinction of the magnetic moment. This assignment that deals with the concept of a charge transfer from Ce^{4+} to Ce^{3+} occurring upon gas charging, within the framework of the Zachariasen–Pauling promotional model, involves the promotion of one electron from the 5d conduction band to a well localized 4f state [72]. The application of this model to the Ce-based systems, like Ce metal, has been strongly questioned by recent *ab initio* electronic structure calculations that show how in α-Ce the unoccupied 4f states are strongly hybridized with the 5d bands. Consequently, it is the competition between the f–f Coulomb interaction and the f–d hybridization that determines the localization of the 4f electrons, the volume and the magnetic state of Ce atoms [67, 72–74].

The results of the present investigation are in full agreement with these calculations, showing direct details of the reduction of the f–d hybridization induced by hydrogen and nitrogen uptake. However, in Ce-based compounds this effect is not enough to determine the localization of the 4f states and the subsequent appearance of a 4f magnetic moment at the Ce sites, as also clearly demonstrated by x-ray circular magnetic dichroism experiments performed at the same absorption edges. The combined interpretation of unpolarized (XAS) and polarized (XCMD) absorption data supports also the hypothesis that the anomalous

strong cell expansion of the Ce-based compounds is linked to the sensitivity of Ce to the hybridization between the 4f and 5d states, directly related to the reduction of the Ce(5d)–Fe(3d) overlap.

Acknowledgments

This work was partially supported by the INFN–CICYT agreement and the Spanish DGICYT MAT93-0240C04 grant. Valuable discussions with J Bartolomé and L M Garcia are gratefully recognized. We wish also to acknowledge T Murata, H Kawata, T Iwazumi and T Miyahara for experimental support at KEK. A special acknowledgment is devoted to H Maruyama and K Kobayashi for their enthusiastic contribution during the experimental runs at KEK and for the clarifying discussion on the XCMD results.

References

[1] Zijlstra H and Westendorp F F 1969 *Solid State Commun.* **7** 857
[2] Buschow K H J, Bouten P C P and Miedema A R 1982 *Rep. Prog. Phys.* **45** 937 and references therein
[3] Wallace W E 1978 *Hydrogen in Metals (Springer Topics in Applied Physics 28)* vol I, ed G Alefeld and J Volkl (Berlin: Springer) and references therein
[4] Buschow K H J 1984 *Handbook on the Physics and Chemistry of Rare Earths* vol 6, ed K A Gschneidner Jr and L Eyring (Amsterdam: North-Holland) and references therein
[5] Wiesinger G and Hilscher G 1991 *Handbook of Magnetic Materials* vol 6, ed K H J Buschow (Amsterdam: Elsevier) and references therein
[6] Yamaguchi M and Akiba E 1994 *Materials Science and Technology* vol 3B, ed R W Cahn, P Haasen and E J Kramer (Weinheim: VCH) and references therein
[7] Sagawa M, Fujimura S, Togawa M, Yamamoto H and Matsuura Y 1984 *J. Appl. Phys.* **55** 2083
[8] Croat J J, Herbst J F, Lee R W and Pinkerton F E 1984 *J. Appl. Phys.* **55** 2078
[9] Buschow K H J 1988 *Handbook of Magnetic Materials* vol 4, ed E P Wohlfarth (Amsterdam: North-Holland) and references therein
[10] Burzo E and Kirchmayr H R 1989 *Handbook on the Physics and Chemistry of Rare Earths* vol 12, ed K A Gschneidner Jr and L Eyring (Amsterdam: North-Holland) and references therein
[11] Herbst J F 1991 *Rev. Mod. Phys.* **63** 819 and references therein
[12] Kirchmayr H R and Poldy C A1979 *Handbook on the Physics and Chemistry of Rare Earths* vol 2, ed K A Gschneidner Jr and L Eyring (Amsterdam: North-Holland) and references therein
[13] Franse J J M and Radwanski R J 1993 *Handbook of Magnetic Materials* vol 7, ed K H J Buschow, (Amsterdam: North-Holland) and references therein
[14] Li H S and Coey J M D 1991 *Handbook of Magnetic Materials* vol. 6, ed K H J Buschow (Amsterdam: North-Holland) and references therein
[15] Buschow K H J 1971 *Phys. Status Solidi* a **7** 199
[16] Givord D and Lemaire R 1974 *IEEE Trans. Magn.* **MAG-10** 109
[17] Gavigan J P, Givord D, Li H S and Voiron J 1988 *Physica* B **149** 345
[18] Mohn P, Wohlfarth E 1987 *J. Phys. F: Met. Phys.* **17** 2421
[19] L'Heritier P, Chaudouet P, Madar R, Rouault A, Senateur J-P and Fruchart R 1984 *C. R. Acad. Sci., Paris* II **299** 849
[20] Oesterreicher K and Oesterreicher H 1984 *Phys. Status Solidi* a **85** K61
[21] Pourarian F, Huang M Q and Wallace W E 1986 *J. Less-Common Met.* **120** 63
[22] Fruchart D, Wolfers P, Vulliet P, Yaouanc A, Fruchart R and L'Heritier P 1986 *Nd–Fe Permanent Magnets. Their Present and Future Applications* ed I V Mitchell (Amsterdam: Elsevier)
[23] Zhang L Y, Pourarian F and Wallace W E 1988 *J. Magn. Magn. Mater.* **71** 203
[24] Neel L 1936 *Ann. Phys., Paris* **5** 232
[25] Zufrowski J, Barnasik A, Krop K, Radwanski R J, Pszczola J, Suwalski J, Kucharski Z and Lukasiak M 1983 *Hyperfine Interact.* **15–16** 801
[26] Rupp B and Wiesinger G 1988 *J. Magn. Magn. Mater.* **61** 269
[27] Wang X Z, Donelly K, Coey J M D, Chevalier B, Etourneau J and Berlureau T 1988 *J. Mater. Sci.* **23** 329
[28] Isnard O, Miraglia S, Soubeyroux J L, Fruchart D and Stergiou A 1990 *J. Less-Common Met.* **162** 273

[29] de Mooij D B and Buschow K H J 1988 *J. Less-Common Met.* **142** 349
[30] Zhong X-P, Radwanski R J, de Boer F R, Jacobs T H and Buschow K H J 1990 *J. Magn. Magn. Mater.* **86** 333
[31] Sun H, Hu B-P, Li H-S and Coey J M D 1990 *Solid State Commun.* **74** 727
[32] Coey J M D and Sun H 1990 *J. Magn. Magn. Mater.* **87** L251
[33] Sun H, Coey J M D, Otani Y and Hurley D P F 1990 *J. Phys. C: Condens. Matter* **2** 6465
[34] Otani Y, Hurley D P F, Sun H and Coey J M D 1991 *J. Appl. Phys.* **69** 5584
[35] Dalmas P de Reotier, Fruchart D, Pontonnier L, Vaillant F, Wolfers P, Yaouanc A, Coey J M, Fruchart R and L'Heritier Ph 1987 *J. Less-Common Met.* **129** 133
[36] Isnard O 1994 *PhD Thesis* J Fourier University
[37] Isnard O, Miraglia S, Kolbeck C, Tomey E, J.L. Soubeyroux, Fruchart D, Guillot M and Rillo C 1992 *J. Alloys Compounds* **178** 15
[38] Isnard O, Miraglia S, Souberyoux J L, Fruchart D, Pannetier J 1992 *Phys. Rev.* B **45** 2920
[39] Fruchart D, Vaillant F, Yaouanc A, Coey J M, Fruchart R, L'Heritier Ph, Riesterer T, Osterwalder J and Schlapbach L 1987 *J. Less-Common. Met.* **130** 97
[40] Miraglia S, Anne M, Vincent H, Fruchart D, Laurant J M and Rossignol M 1989 *J. Less-Common Met.* **153** 51
[41] Isnard O, Miraglia S, Soubeyroux J L, D. Fruchart and Stergiou A 1990 *J. Less-Common Met.* **162** 273
[42] Isnard O, Miraglia S, Fruchart D and Deportes J 1992 *J. Magn. Magn. Mater.* **103** 157
[43] Isnard O, Miraglia S, Kolbeck C, Tomey E, Soubeyroux J L, Fruchart D, Guillot M and Rillo C 1992 *J. Alloys Compounds* **178** 15
[44] Chaboy J 1991 *PhD Thesis* Zaragoza University
[45] Chaboy J, Garcia J, Marcelli A, Isnard O, Miraglia S and Fruchart D 1992 *J. Magn. Magn. Mater.* **104–107** 1171
[46] Capehart T W, Mishra R K, Meisner G P, Fuerst C D and Herbst J F 1993 *App. Phys. Lett.* **63** 3642
[47] Buschow K H J and van Diepen A M 1976 *Solid State Commun.* **19** 79
[48] Chaboy J, Garcia J and Marcelli A 1992 *J. Magn. Magn. Mater.* **104–107** 661
[49] Chaboy J, Marcelli A, Garcia L M, Garcia J, Maruyama H, Kobayashi K and Bozukov L 1994 *Solid State Commun.* **91** 769
[50] Chaboy J, Marcelli A and Bozukov L 1993 *Japan. J. Appl. Phys.* **32** 758
[51] Chaboy J, Marcelli A, Bozukov L, Baudelet F, Dartyge E, Fontaine A and Pizzini S 1995 *Phys. Rev.* B **51** 9005
[52] Chaboy J, Marcelli A, Garcia L M, Bartolome J, Kuzmin M, Maruyama H, Kobayashi K, Kawata H and Iwazumi T 1994 *Europhys. Lett.* **28** 135
[53] See for example,
Sayers D E and Bunker B A 1988 *X-ray Absorption: Principles, Applications, Techniques of EXAFS, SEXAFS and XANES* ed D C Koningsberger and R Prins (New York: Wiley) ch 6
[54] Bianconi A 1988 *X-ray Absorption: Principles, Applications, Techniques of EXAFS, SEXAFS and XANES* ed D C Koningsberger and R Prins (New York: Wiley) ch 11 and references therein
[55] Andreev A V, Deryagin A V, Kudrevatykh N V, Mushnikov N V, Reimer V A and Terent'ev S V 1986 *Sov. Phys.–JETP* **63** 608
[56] Kuijpers F A 1973 *Philips Res. Rep. Suppl.* **2**
[57] Yelon W B and Herbst J F 1986 *J. Appl. Phys.* **59** 93
For a review, see also [9–11].
[58] Buschow K H J and Van J S Wieringen 1970 *Phys. Status Solidi* **42** 231
For a review, see also [12–13].
[59] Materlik G, Müller J E and Wilkins J W, 1983 *Phys. Rev. Lett.* **50** 267
[60] Müller J E and Wilkins J W 1984 *Phys. Rev.* B **29** 4331
[61] Materlik G, Sonntag B and Tausch M 1983 *Phys. Rev. Lett.* **51** 1300
[62] Schütz G, Wagner W, Wilhelm W, Kienle P, Zeller R, Frahm R and Materlik G 1987 *Phys. Rev. Lett.* **58** 737
For a review, see
Lovesey S W 1993 *Rep. Prog. Phys.* **56** 257
[63] Brouder C and Hikam M 1991 *Phys. Rev.* B **43** 3089
[64] Johanson B, Nordström L, Eriksson O and Brooks M S S 1991 *Phys. Scr.* T **39** 100
[65] Campbell I A 1972 *J. Phys. F: Met. Phys.* **2** L47
[66] Giorgetti C, Pizzini S, Dartyge E, A. Fontaine, Baudelet F, Brouder C, Bauer Ph, Krill G, Miraglia S, Fruchart D and Kappler J P 1993 *Phys. Rev.* B **48** 12 732

[67] Szotek Z, Temmerman W M and Winter H 1994 *Phys. Rev. Lett.* **72** 1244
[68] Harmon B N and Freeman A J 1974 *Phys. Rev.* B **10** 1979
[69] Wang X, Lueng T C, Harmon B N and Carra P 1993 *Phys. Rev.* B **47** 9087
[70] Lang J C, Wang X, Antropov V P, Harmon B N, Goldman A I, Wan H, Hadjipanayis G C and Finkelstein K D 1994 *Phys. Rev.* B **49** 5993
[71] Nördstrom L, Eriksson O, Brooks M S S and Johansson B 1990 *Phys. Rev.* B **41** 911
[72] Zachariasen W H, quoted by
Lawson A W and Tang T Y 1949 *Phys. Rev.* **76** 301
Pauling L, quoted by
Schuck A F and Sturdivant J H 1950 *J. Chem. Phys.* **18** 145
[73] Eriksson O, Nördstrom L, Brooks M S S and Johansson B 1988 *Phys. Rev. Lett.* **60** 2523
[74] Eriksson O, Brooks M S S and Johanson B 1990 *Phys. Rev.* B **41** 7311
[75] Svane A 1994 *Phys. Rev. Lett.* **72** 1248
[76] Stähler S, Schütz G and Ebert H 1993 *Phys. Rev.* B **47** 818
[77] Pizzini S, Fontaine A, Dartyge E, Giorgetti C, Baudelet F, Kappler J P, Boher P and Giron F 1994 *Phys. Rev.* B **50** 3779